

2011

Inkjet and extrusion printing of conducting poly(3,4-ethylenedioxythiophene) tracks on and embedded in biopolymer materials

Charles A. Mire
cm482@uow.edu.au

Animesh Agrawal
University Massachusetts Dartmouth

Gordon G. Wallace
University of Wollongong, gwallace@uow.edu.au

Paul Calvert
University of Wollongong, pcalvert@uow.edu.au

Marc in het Panhuis
University of Wollongong, panhuis@uow.edu.au

Publication Details

Mire, C. A., Agrawal, A., Wallace, G. G., Calvert, P. & in het Panhuis, M. (2011). Inkjet and extrusion printing of conducting poly(3,4-ethylenedioxythiophene) tracks on and embedded in biopolymer materials. *Journal of Materials Chemistry*, 21 (8), 2671-2678.

Inkjet and extrusion printing of conducting poly(3,4-ethylenedioxythiophene) tracks on and embedded in biopolymer materials

Abstract

Two printing methods, extrusion and inkjet, are used to deposit tracks of PEDOT/PSS conducting polymer onto biopolymer films with a view to prepare implantable tissue mimics containing electronic devices. Extruded tracks offer lower printing resolution, but better electrical characteristics compared to inkjet printed tracks. The biopolymer-ink interaction results in narrower printed tracks compared to those on glass. This affects the final conductivity, which is lower for printed tracks on biopolymer than for lines printed on glass, due to the part of the track lying below the surface. Extrusion printing is used to embed tracks into a biopolymer matrix, resulting in significant improvement in electrical characteristics. The electrical conductivity of embedded tracks (17 S cm^{-1}) is an order of magnitude higher than for track deposition on the surface of biopolymer film and 3 times higher than for tracks on glass.

Keywords

3, inkjet, extrusion, 4, conducting, printing, ethylenedioxythiophene, poly, tracks, biopolymer, embedded, materials

Disciplines

Life Sciences | Physical Sciences and Mathematics | Social and Behavioral Sciences

Publication Details

Mire, C. A., Agrawal, A., Wallace, G. G., Calvert, P. & in het Panhuis, M. (2011). Inkjet and extrusion printing of conducting poly(3,4-ethylenedioxythiophene) tracks on and embedded in biopolymer materials. *Journal of Materials Chemistry*, 21 (8), 2671-2678.

Inkjet and extrusion printing of conducting poly(3,4-ethylenedioxythiophene) tracks on and embedded in biopolymer materials†

Charles A. Mire,^{ab} Animesh Agrawal,^c Gordon G. Wallace,^b Paul Calvert^{*c} and Marc in het Panhuis^{*ab}

Received 22nd October 2010, Accepted 3rd December 2010

DOI: 10.1039/c0jm03587d

Two printing methods, extrusion and inkjet, are used to deposit tracks of PEDOT/PSS conducting polymer onto biopolymer films with a view to prepare implantable tissue mimics containing electronic devices. Extruded tracks offer lower printing resolution, but better electrical characteristics compared to inkjet printed tracks. The biopolymer–ink interaction results in narrower printed tracks compared to those on glass. This affects the final conductivity, which is lower for printed tracks on biopolymer than for lines printed on glass, due to the part of the track lying below the surface. Extrusion printing is used to embed tracks into a biopolymer matrix, resulting in significant improvement in electrical characteristics. The electrical conductivity of embedded tracks (17 S cm^{-1}) is an order of magnitude higher than for track deposition on the surface of biopolymer film and 3 times higher than for tracks on glass.

Introduction

There are many potential medical applications for implantable electronic devices, including sensors, controllable drug release systems, and stimulation systems for nerves or muscles. There is a problem in matching the high modulus and fatigue sensitivity of metallic conductors to the low modulus and mobility of tissues. To date, devices such as pacemakers and the artificial cochlea are implanted in regions of limited motion, but fatigue cracking can still be a problem. Accordingly, we are seeking to develop flexible electrode materials with elastic moduli comparable to tissues, porosity to allow flow of interstitial fluids, and resistance to fracture under repeated stretching and bending. Ideally, such conductors will also be capable of rugged attachment to rigid encapsulated electronics located at low mobility sites. We envisage both fine, higher resistance leads for sensor connections and larger low resistance leads for carrying higher currents to actuators.

Conducting polymers have been deposited on hard surfaces, such as polyester and glass, and on porous papers.^{1,2} They have

also been combined with hydrogels in an effort to make more elastic conductors.^{3,4} In this work, we report on the properties of conducting polymer lines printed into hydrogels, since these embedded conductors should yield biocompatible conductors meeting the requirements outlined above. Printing onto a porous substrate results in a composite structure combining the properties of the substrate and conductor, as shown previously by conducting polymers on textiles.⁵ The current paper describes for the first time printing conducting tracks onto and into gels.

The selected hydrogel matrix is a complex of chitosan and hyaluronic acid formed by pH shift during evaporation of acid and water from a mixed solution. Previous studies of this complex monitored gelation by a change in solution conductance, and showed (by infrared spectroscopy) that the hyaluronic acid is largely ionized.⁶ Swelling studies of films with increasing amounts of chitosan showed that a large excess of chitosan resulted in modest increases in swelling in water.⁷ Moduli of films formed through layer-by-layer processes have been determined by atomic force microscopy on both native and chemically cross-linked films.⁸ Such gels have been studied as scaffolds for the growth of skin cells including fibroblasts and keratinocytes.^{9,10}

The conducting lines were formed from the water soluble polymer, poly(3,4-ethylenedioxythiophene)/poly(sodium 4-styrene-sulfonate) (PEDOT/PSS). This conducting polymer has been widely characterized as a conductor. Electrodes of PEDOT/PSS have been used for neural communication,^{11–13} and have been shown to be quite stable in a biological environment.¹⁴

The conductors were deposited on biopolymer substrates both by syringe extrusion of a thick paste to form thick lines and by inkjet printing of a dilute suspension to make thin lines. We then described the morphology and electrical characteristics of these lines printed onto biopolymers and compared them to glass.

^aSoft Materials Group, School of Chemistry, University of Wollongong, Wollongong, Australia. E-mail: panhuis@uow.edu.au; Fax: +61 24221 4287; Tel: +61 24221 3155

^bARC Centre of Excellence for Electromaterials Science, Intelligent Polymer Research Institute, University of Wollongong, Wollongong, Australia

^cDepartment of Materials and Textiles, University of Massachusetts Dartmouth, North Dartmouth, MA, 02747, USA. E-mail: pcalvert@umassd.edu; Tel: +1 5052756037

† Electronic supplementary information (ESI) available: Microscopy of extrusion and inkjet printed tracks on the surface of biopolymer film, microscopy of attempts to embed tracks and stress–strain curve of biopolymer with embedded tracks. See DOI: 10.1039/c0jm03587d

Since the printed fluid can interact with the biopolymer substrate, line shapes and electrical characteristics are different from those deposited onto a hard surface. Extrusion printing was chosen to embed tracks into a biopolymer. This revealed that the conductivity of embedded tracks is several times higher than for tracks on glass, and an order of magnitude higher than tracks on the surface of biopolymer films.

Experimental

Materials

Medium molecular weight chitosan (CH, batch 04609LD, degree of deacetylation 79%, molecular weight range $1.9\text{--}3.1 \times 10^5 \text{ g mol}^{-1}$), poly(sodium 4-styrene-sulfonate) (PSS, $M_w = 70\,000 \text{ g mol}^{-1}$), iron(III) perchlorate, lactic acid, and dialysis tubing cellulose membrane (retaining most material with molecular weight greater than $12\,000 \text{ g mol}^{-1}$) were purchased from Sigma-Aldrich and used as received. Hyaluronic acid, sodium salt (HA), was purchased from Fluka, while sodium hydroxide, acetic acid (glacial), and ammonium persulfate (APS) were obtained from Ajax. 3,4-Ethylenedioxythiophene (EDOT) was sourced from Bayer, and distilled prior to use. Adhesive copper tape and high purity silver paint were purchased from 3M and SPI Supplies, respectively. Milli-Q water (resistivity $18 \text{ M}\Omega \text{ cm}$) was used for all solutions.

Biopolymer solution and substrate preparation

CH solutions were prepared using established protocols^{15,16} (with minor modifications). CH–HA solutions were prepared by first dissolving HA in water (0.25 mg mL^{-1} , under stirring at $50 \text{ }^\circ\text{C}$), followed by addition of acetic acid (1% v/v) and CH (20 mg mL^{-1} under stirring at $70 \text{ }^\circ\text{C}$). CH solutions were prepared by dissolving CH (30 mg mL^{-1}) in 1% v/v acetic acid, and stirred until dissolved at $90 \text{ }^\circ\text{C}$.

Supported biopolymer substrates were prepared by coating glass microscope slides with biopolymer solutions through evaporative casting of a fixed volume of solution under controlled ambient conditions ($21 \text{ }^\circ\text{C}$, 45% relative humidity).

Freestanding biopolymer substrates were prepared by an evaporative casting process of biopolymer solutions on Teflon coated substrates under controlled ambient conditions. The films were then peeled off the substrate to yield uniform freestanding films.

The resulting thicknesses were $16 \pm 3 \text{ }\mu\text{m}$ and $21 \pm 3 \text{ }\mu\text{m}$ for the supported and freestanding biopolymer films, respectively. All films were clear with a 93% transmittance over the wavelength range 400–800 nm.

Synthesis of PEDOT/PSS

PEDOT/PSS was synthesized following an established procedure.¹⁷ In short, an aqueous solution of PSS ($235 \text{ }\mu\text{M}$) was degassed in a sonicating bath. EDOT was added dropwise to the solution, at an EDOT : PSS mass ratio of 1 : 2.5, and was further degassed until clear, followed by stirring for 30 min. 200 mL of an APS solution (260 mM) was added under stirring, followed by dropwise addition of iron(III) perchlorate as catalyst. The

solution was stirred for 12 h to allow polymerisation, followed by purification by dialysis against water for 24 h.

Rheology

Biopolymer and ink flow curves (apparent viscosity and shear stress as a function of shear rate) were determined using an Anton Paar Physica MCR 301 rheometer (PP25 head) at $20 \text{ }^\circ\text{C}$.

Extrusion printing

Extrusion printing was carried out using two custom-built syringe-controlled deposition systems consisting of an Asymtek Automove 402 Dispensing System, or a Sherline 8020 CNC milling stage, each with programmable *xyz*-motion. Both deposition systems were fitted with a 5 mL syringe with a Luer lock $100 \text{ }\mu\text{m}$ needle, which is pressurized using nitrogen gas.¹⁸ The lateral motion ($\sim 1 \text{ cm s}^{-1}$) is balanced to the extrusion rate as determined by the air pressure (30–40 psi) and ink viscosity.

The viscous PEDOT/PSS dispersion (concentration 36.8 mg mL^{-1}) was prepared by centrifuging the PEDOT/PSS dispersion at 3000g for 110 min, followed by removal of the supernatant. PEDOT/PSS tracks (length 2 cm, 1 layer) were deposited onto glass and biopolymer (supported and freestanding) substrates using syringe-controlled deposition. Embedded tracks (length up to 20 cm, 1 layer) were deposited by positioning the syringe needle 1 mm beneath the surface of a biopolymer solution (CH–HA or CH) and extruding as normal. The solution with embedded tracks was allowed to dry for 24 hours under ambient conditions, and peeled off to yield uniform freestanding biopolymer films with embedded tracks.

Inkjet printing

PEDOT/PSS dispersions (concentration 18.4 mg mL^{-1} , temperature $25 \text{ }^\circ\text{C}$, and surface tension 27 mN m^{-1}) were inkjet printed using a Dimatix DMP inkjet printing system (FujiFilm Dimatix).^{19,20} The cartridges used for printing were MEMS-based, with 16 nozzles ($20 \text{ }\mu\text{m}$ diameter) spaced at $254 \text{ }\mu\text{m}$, each dispensing a droplet volume of 10 pL. Surface tension was determined using a Dataphysics OCA 20 goniometer (pendant drop method). Several adjustments to the default settings were made, the piezoelectric nozzle voltage and jetting frequency were optimised such that the ejected drops were spherical in shape prior to hitting the substrate, as well as using only 1 cartridge nozzle during deposition. This enabled reliable inkjet deposition of lines consisting of a single row of drops. PEDOT/PSS tracks (length 2 cm, up to 45 layers) were printed using $30 \text{ }\mu\text{m}$ resolution (dot spacing = 333 dots per cm^2 or 847 dots per inch) onto biopolymer and glass substrates.

Electrical characterisation

Conductivity measurements of PEDOT/PSS films, for comparison with printed tracks, were carried out using a JANDEL four-point probe resistivity system (model RM2). Film thickness was determined using a Mitutoyo digital micrometer. For conductivity measurements PEDOT/PSS tracks were contacted with conducting silver paint. Current (*I*)–voltage (*V*) characteristics were determined under controlled ambient conditions in air

(21 °C, 45% relative humidity), using a waveform generator (Agilent 33220A) interfaced with a digital multimeter (Agilent 34410A).

Mechanical characterisation

Tensile testing on freestanding biopolymer films was done with a Shimadzu Compact Tabletop EZ-S Series EZ Test tensile tester with a 50 N load cell at a strain rate of 1% per min. Samples were mounted on aperture cards (10 mm length window). The paper windows were cut once the sample was mounted in the instrument.

Track morphology

The width and thickness of inkjet and extrusion printed PEDOT/PSS tracks on the biopolymer and glass substrates were measured using atomic force microscopy (AFM) and contact profilometry. Inkjet printed tracks on the supported-biopolymer substrate were imaged in air using an AFM (Asylum Research MFP-3D Atomic Force Microscope), in tapping mode with a 40 N m⁻¹ silicon cantilever, at a scan rate of 0.5 Hz. All other tracks on the biopolymer (supported and freestanding) and glass substrates were measured using a contact profilometer (Veeco Dektak 150 with a 12.5 μm tip and 5.00 mg force).

Embedded tracks were characterised by scanning electron microscopy (SEM) and energy dispersive spectroscopy (EDS), which were performed using a JEOL JSM-7500FA. Cross-sections of the embedded tracks were prepared by freezing in liquid nitrogen, followed by mechanical treatment.

Optical microscopy and image analysis (LEICA DFC290 optical microscope coupled to LEICA Application Suite software) were used to image all tracks.

Results and discussion

Ink rheology

The flow curves for the two PEDOT/PSS inks are shown in Fig. 1. Both dispersions display shear thinning behaviour, *i.e.* viscosity (η) decreases with increasing shear rate (s) which could be fitted to the well-known power-law model,²¹

$$\eta = Ks^n \quad (1)$$

where K and n indicate the ‘consistency’ and power law index, respectively. It is interesting to note that a doubling in the concentration of the PEDOT/PSS ink results in a large increase in the apparent viscosity. For example, at a shear rate of 10 s⁻¹ the viscosity of the concentrated ink is 12 600 mPa s compared to 60 mPa s observed for the less concentrated ink. It is likely that this large difference in viscosity can be attributed to the well-known effect of polymer entanglement, *i.e.* the concentration of the viscous PEDOT/PSS is above the coil overlapping concentration.^{21,22} In addition, the ‘consistency’ of the inks differs by 2 orders of magnitude (Table 1). The K values of well-known materials can be used to bring our values into perspective. Molten chocolate ($K = 50\,000$ mPa s) exhibits a similar value to that obtained for the concentrated ink, while the other ink is similar to K values observed for synovial fluids.²¹

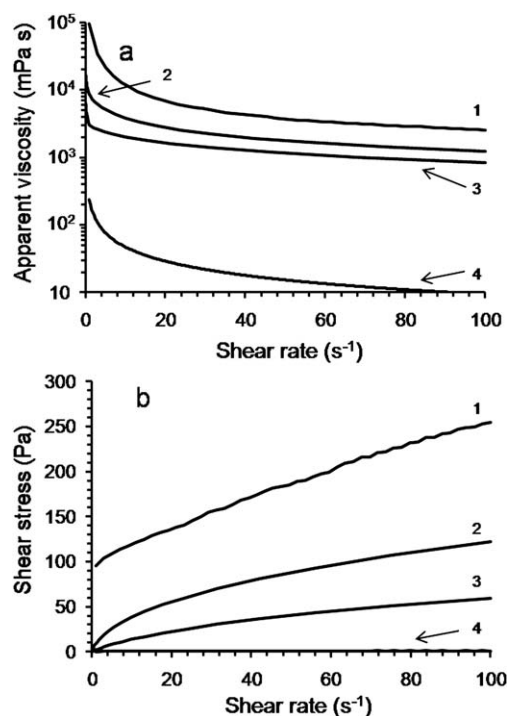


Fig. 1 Flow curves for biopolymers and inks. (a) Apparent viscosity and (b) shear stress as a function of shear rate. Numbers 1–4 indicate concentrated ink, CH, CH–HA and less concentrated ink, respectively.

Fig. 1b shows that the concentrated ink exhibits a yield point, *i.e.* the sample starts to flow only when a certain amount of force is applied. This point can be determined using the Bingham model:

$$\tau = \tau_B + \eta_B s \quad (2)$$

where τ_B and η_B indicate the Bingham yield point and Bingham flow coefficient, respectively. Although, the values obtained using the Bingham model are dependent on the shear rate range it provides a good approximation for the determination of yield points. The model shows that the concentrated ink follows the Bingham model over a wide shear rate range (0.01–100 s⁻¹) with $\tau_B = 105$ Pa, whereas the less concentrated ink exhibits $\tau_B = 0.44$ for a shear rate range of 10–100 s⁻¹. Similar differences are observed for the Bingham flow coefficient.

The large differences in the viscosity, ‘consistency’ and the Bingham yield point values of the two PEDOT/PSS are consistent with our inability to either inkjet print the more concentrated ink or extrusion print the less concentrated ink.

Extrusion on glass vs. supported biopolymer

Five parallel PEDOT/PSS tracks were deposited onto glass or supported-hydrogel substrates (Fig. S1†). Water diffusion into the biopolymer and pH changes would be expected to affect the shape and microstructure of the PEDOT/PSS written on the gel as opposed to glass. Fig. 2a and b show that the width of extrusion printed tracks on glass and biopolymer substrates is 522 ± 22 μm and 180 ± 10 μm, respectively. Profilometry measurements showed that PEDOT/PSS tracks on the

Table 1 Summary of rheology analysis of biopolymer solutions (CH–HA and CH) and PEDOT/PSS dispersions with concentrations of 20.25 mg mL⁻¹ (CH–HA), 30 mg mL⁻¹ (CH), 18.4 mg mL⁻¹ (Ink solution) and 36.8 mg mL⁻¹ (Viscous ink). ‘Consistency’ (K) and power law index (n) values were obtained through curve fitting with the power law model, eqn (1). Bingham yield point (τ_B) and Bingham flow coefficient (η_B) values were obtained using the Bingham model, eqn (2). Note: τ_B values for viscous ink determined a shear rate range of 0.01–100 s⁻¹, while values for all other samples were obtained at a shear rate range of 10–100 s⁻¹. CH and HA indicate chitosan and hyaluronic acid, respectively

Sample	$K/\text{mPa s}$	n	τ_B/Pa	$\eta_B/\text{Pa s}$
Ink solution	423 ± 13	-0.85 ± 0.01	0.44 ± 0.06	0.040 ± 0.007
Viscous ink	68516 ± 282	-0.74 ± 0.01	105 ± 1	1.57 ± 0.02
CH–HA	2327 ± 5	-0.27 ± 0.01	13.5 ± 1.6	0.49 ± 0.03
CH	7313 ± 26	-0.31 ± 0.01	39 ± 3	0.88 ± 0.06

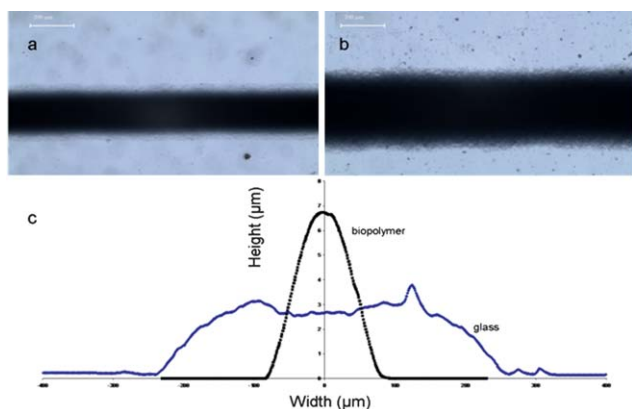


Fig. 2 Optical microscopy of extrusion printed PEDOT/PSS tracks on (a) supported-biopolymer substrate and (b) glass substrate. (c) Cross-sectional profiles of tracks on supported-biopolymer (black) and glass (blue) substrates.

biopolymer substrate are higher, but narrower compared to the tracks deposited onto glass slides (Fig. 2c).

As evidence for mass transfer between the viscous PEDOT/PSS paste and the hydrogel, drop shape analysis shows that the contact angle of PEDOT/PSS with the CH–HA substrate decreased over 5 min from 111° to 68°. In contrast, the contact angle of a PEDOT/PSS drop with the glass substrate remained constant over 5 min at 30°.

Analysis of the cross-sectional area (Fig. 2c, areas under the curve) revealed that the tracks on the biopolymer substrate have a smaller cross-sectional area than those on the glass substrate. The values for extrusion printed tracks on biopolymer and glass are 620 ± 80 μm² and 1220 ± 150 μm², respectively. However, the extrusion printer deposits the same amount of material onto each of the substrates. The difference in cross-sectional areas suggests that either the PEDOT/PSS density is different after drying on the biopolymer substrate or that the line is partly below the surface, which was confirmed by SEM and EDS analyses (Fig. 3).

Elemental analysis by EDS of the cross-sectional area revealed that the carbon, sulfur and sodium responses are different for the track area above and below the surface. The PSS counterion Na⁺ is present in the track above the surface (area 1, Fig. 3c), but cannot be detected anywhere below. Immediately below the surface (area 2, Fig. 3c), the S intensity (present in both PEDOT and PSS) has decreased by 65% of that observed for the track above the surface (area 1, Fig. 3c). At a distance between 4 and 7 μm below the surface (area 3, Fig. 3c), this intensity has reduced

even further, with only 14% remaining. In contrast, the C intensity (present in PEDOT/PSS and biopolymer) shows a 2.5- and 3.75-fold increase in areas 2 and 3, respectively, compared to the track above the surface. This clearly demonstrates that part of the PEDOT/PSS line is below the surface and is mixed with the biopolymers.

The current–voltage (I – V) characteristics were investigated under controlled ambient conditions (21 °C, 45% relative humidity). All tracks exhibited Ohmic behaviour with linear I – V characteristics (Fig. 4a). Printing up to five tracks and connecting

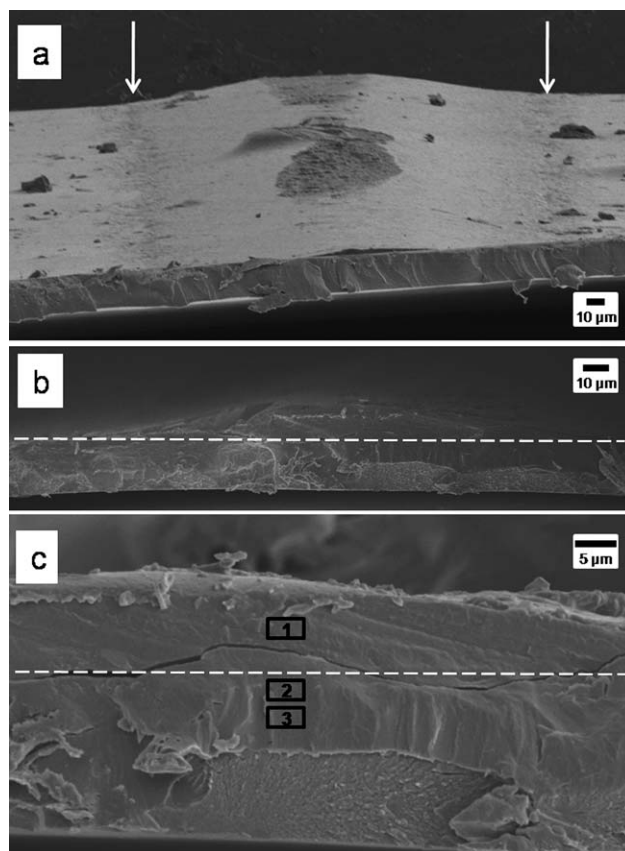


Fig. 3 Scanning electron microscopy (SEM) images of extrusion printed PEDOT/PSS tracks on a freestanding biopolymer substrate. (a) Top view of a cross-section prepared by freezing in liquid nitrogen followed by mechanical treatment. Arrows indicate edge of the track on the surface. (b and c) Enlarged views of cross-sectional area. Dotted line indicates the surface of the freestanding film. Squares 1–3 indicate areas of analysis for energy dispersive spectroscopy.

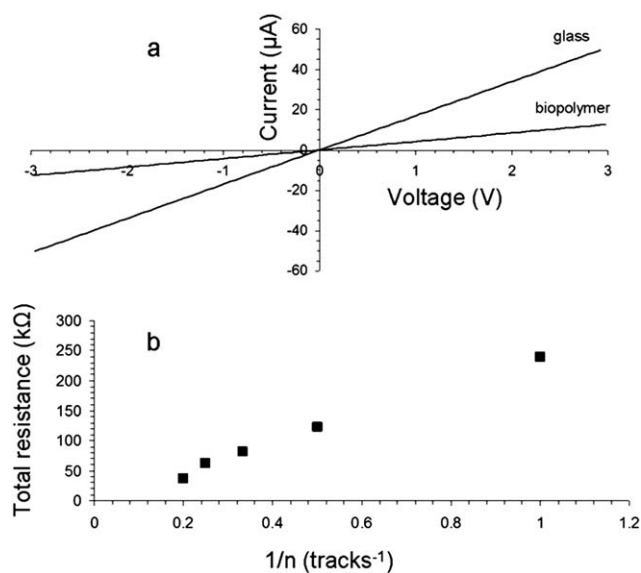


Fig. 4 Electrical characteristics of PEDOT/PSS tracks printed onto the supported-biopolymer substrate. (a) Current–voltage (I – V) characteristics of extrusion printed tracks on supported-biopolymer and glass substrates (one track with channel length 2 cm). (b) Total resistance *versus* inverse of number of extruded parallel tracks (channel length 2 cm). All measurements were carried out under controlled ambient conditions (21 °C, 45% RH).

them in parallel give the expected decrease in resistance with number of tracks, showing that the resistance is very reproducible (Fig. 4b). A single track (length = 2 cm, 1 layer) onto the glass substrate results in a resistance of 30 kΩ cm⁻¹, while extrusion printing on the biopolymer substrate results in a higher resistance (120 kΩ cm⁻¹). These resistance values represent the total resistance (R_T) and include the contact resistance (R_C), *i.e.*

$$R_T = \frac{l}{\sigma A} + R_C \quad (3)$$

where l , σ and A indicate the sample's length, DC conductivity and cross-sectional area, respectively. Previously, it has been shown that the contact resistance for similar systems with painted silver contacts was less than 1 kΩ and can be ignored for conductivity estimates.^{23,24} The DC conductivity of the extruded tracks can then be evaluated using $\sigma \approx l/(R_T A)$. This yields a conductivity value of 2.8 ± 0.4 S cm⁻¹ on glass, while a film prepared by evaporative casting on glass yielded 2.1 ± 0.7 S cm⁻¹. If we revise the cross-sectional area of the tracks printed on the supported biopolymer by taking into account what lies beneath the surface, we get a revised conductivity of 0.7 ± 0.1 S cm⁻¹. These conductivity values are in good agreement with the reported conductivity range (0.4–10 S cm⁻¹) for untreated PEDOT/PSS films.^{25–27}

Inkjet printing on supported biopolymer

In inkjet printing the drop spacing requires careful optimisation, as placing the drops too close together may result in unwanted wetting effects due to ink–substrate interactions. Placing the drops too far apart can result in printed features consisting of disconnected drops. For example, inkjet printing a single row

of PEDOT/PSS drops with 250 drops per cm (dpcm) on glass is not sufficient to yield continuous tracks (Fig. S2a†). Since each 10 pL drop produces a circle of ink 40 µm in diameter, continuous tracks require a resolution of at least 333 dpcm (Fig. S2b†). Inkjet printing PEDOT/PSS (15 layers, 333 dpcm) onto a polylactic acid–poly(glycolide-*co*-lactide), which has a higher contact angle, did not result in continuous tracks (Fig. S2c†).

Up to 45 layers of continuous PEDOT/PSS tracks were inkjet printed on the glass and CH–HA substrates (Fig. 5). Deposition of 15 and 45 layers on the hydrogel substrate results in a height of 1.31 ± 0.04 µm and 3.12 ± 0.04 µm, respectively. The average height over the first 15 layers is 88 nm per layer. However, the following additional 30 layers result in an increase in a height of 2.79 µm or 60 nm per layer. The difference may reflect the lateral spreading of the lines as they build up. In comparison, deposition of 15 layers on glass results in a height 0.62 ± 0.10 µm or 40 nm per inkjet printed layer. The width of PEDOT/PSS tracks (15 layers) on glass and biopolymer substrates is 113 ± 11 µm and 50 ± 5 µm, respectively. Analysis of the cross-sectional area according to profilometry (Fig. 5f), gives values for 15 printed tracks on biopolymer and glass as 41 ± 2 µm² and 49 ± 2 µm², respectively. As with the extruded lines, those on the biopolymer substrate have less material above the surface than those on the glass substrate. The difference in track morphology observed on glass and biopolymer substrate is similar to what was observed for extrusion printing tracks, *i.e.* higher, but narrower.

The I – V characteristics were investigated under controlled ambient conditions (21 °C, 45% RH). Several layers of drops must be deposited before the track becomes electrically conducting (Fig. 6a). The electrical resistance (R_T) of 5 inkjet printed layers is 6.1 MΩ, whereas this decreases to 2.0 MΩ for 10 layers.

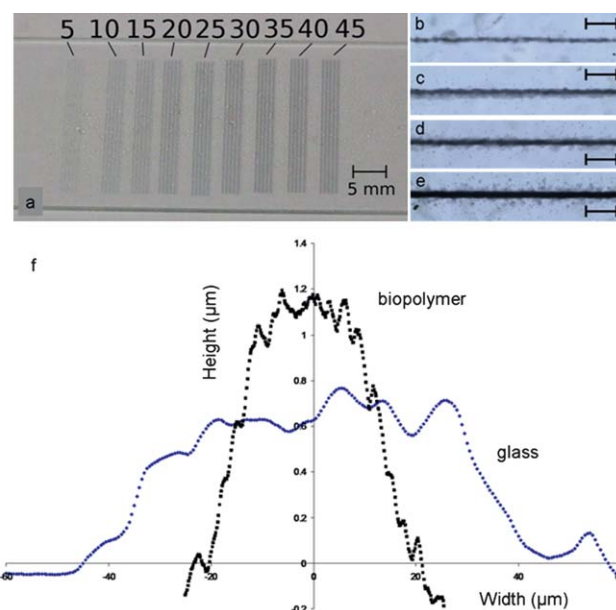


Fig. 5 Optical microscopy of (a) PEDOT/PSS tracks inkjet printed (resolution 333 dpcm) onto the supported-biopolymer substrate. Numbers indicate number of inkjet printed layers. (b–e) Enlarged view of 5, 10, 15 and 45 inkjet printed layers, respectively. Scale bars represent 200 µm (f) cross-sectional profiles of 15 inkjet printed layers of PEDOT/PSS on supported-biopolymer (black) and glass (blue) substrates.

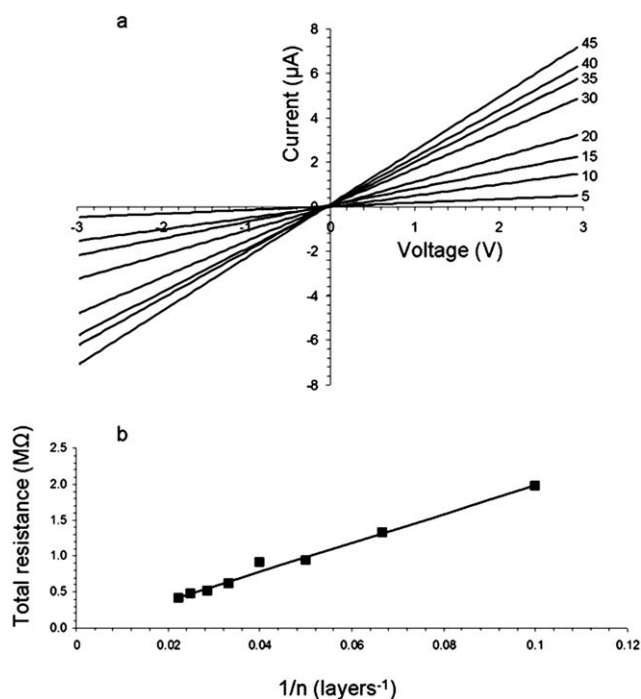


Fig. 6 Electrical characteristics of PEDOT/PSS tracks inkjet printed onto the supported-biopolymer substrate. (a) Current–voltage characteristics of inkjet printed tracks (channel length 2 cm), numbers indicate number of inkjet printed layers. (b) Total resistance *versus* inverse of number of inkjet printed layers (10–45 layers). The straight line is a fit to eqn (3).

As shown by the straight line in Fig. 6b, the electrical resistance of inkjet printed tracks is inversely proportional between 10 and 45 printing cycles, showing that the buildup of inkjet printed material is uniform with a resistance of $207 \text{ k}\Omega \text{ cm}^{-1}$ for 45 layers. This yields a conductivity value of $0.93 \pm 0.12 \text{ S cm}^{-1}$, and a revised conductivity value of $0.21 \pm 0.05 \text{ S cm}^{-1}$ (taking into account what lies beneath the surface).

The remainder of this article focusses on embedding conducting tracks in a gel matrix. It should be clear that extrusion printing offers a number of advantages over inkjet printing, *i.e.* it is relatively straightforward to embed a large amount of ink (in a single pass), by locating the syringe needle below the surface of a gel bath and practically useful track conductivity can be achieved.

Embedding tracks in a biopolymer matrix

In order to extrude lines into biopolymer, a more viscous biopolymer with a higher yield point than the CH–HA solution used for film casting was required. As shown in Table 1, increasing the concentration of chitosan, but omitting the hyaluronic acid increases the yield point. Fig. 7 shows that this had the desired effect on our capability for embedding tracks, *i.e.* it was straightforward to produce tracks of up to 20 cm in length (limited only by the length of our biopolymer solution bath).

The mechanical characteristics of biopolymer films were not significantly affected by the embedded tracks. The tensile strength, Young's modulus and strain values of biopolymer films

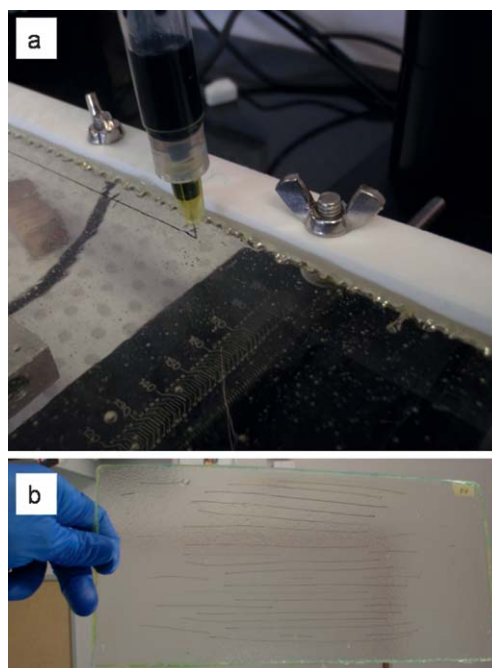


Fig. 7 (a) Photograph of extrusion of PEDOT/PSS into the biopolymer solution. (b) Photograph of biopolymer matrix with embedded tracks.

with and without embedded tracks were approximately 80 MPa, 1700 MPa and 16%, respectively (Fig. S4†).

The I – V characteristics of the embedded tracks were investigated under controlled ambient conditions. All tracks exhibited Ohmic behaviour (Fig. 8a) with the electrical resistance proportional to track length. The average resistance of all printed tracks with lengths between 0.45 cm and 12.0 cm is $4.7 \pm 1.6 \text{ k}\Omega \text{ cm}^{-1}$. SEM analysis (Fig. 8b and c) suggests that the cross-sectional area of embedded tracks is $1228 \pm 120 \mu\text{m}^2$, which yields a conductivity value of $17 \pm 7 \text{ S cm}^{-1}$. The corresponding values for extruded tracks on glass and freestanding biopolymer substrates are $6.3 \pm 1.1 \text{ S cm}^{-1}$ and $1.7 \pm 0.4 \text{ S cm}^{-1}$.

For tracks produced using the first batch of PEDOT/PSS the ratio of conductivity for tracks on glass : supported biopolymer is 1 : 0.25. Whereas for the second batch of PEDOT/PSS the ratios for tracks on glass : freestanding biopolymer : embedded yields 1 : 0.27 : 2.7.

The fact that the conductivity of PEDOT/PSS embedded into the biopolymer is almost 3 and 10 times larger than on glass and on the surface of a freestanding biopolymer, respectively, possibly reflects the effect of the drying conditions on connectivity of the PEDOT nanoparticles. It is also clear that there is a significant effect on resistance, due to the drying of the biopolymer in the preparation of the embedded tracks. The resistance of the embedded tracks is more than an order of magnitude lower compared to tracks deposited onto biopolymer substrates. Effects of processing and annealing conditions on conductivity of PEDOT films have been widely reported.^{28,29}

Conclusions

Conducting tracks embedded in hydrogels could function as flexible, biocompatible conductors for implanted sensors, controlled drug delivery systems and other devices. Cells can be

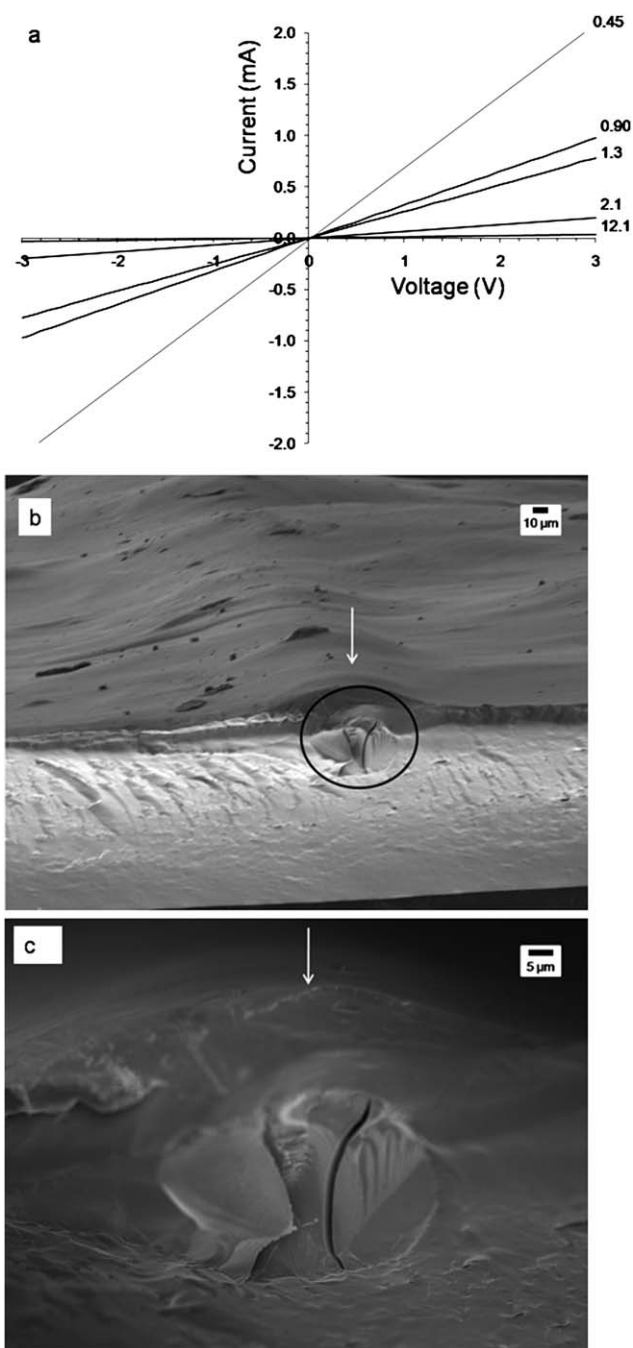


Fig. 8 Embedded PEDOT/PSS tracks. (a) Current–voltage characteristics of inkjet printed tracks, numbers indicate channel length (in cm). (b) Scanning electron microscopy image of the cross-sectional area of an embedded track. Ellipsoidal and arrow indicate the track and surface of the film, respectively. (c) Enlarged view of the cross-sectional area.

grown on the surface of many conducting polymers,^{30–32} showing that they have a high degree of biocompatibility.

Of the two printing methods studied here, inkjet printing of dilute suspensions provides finer resolution and better deposition control, allowing lines to be formed with resistances of a few hundred $\text{k}\Omega \text{ cm}^{-1}$ and linewidths of $50 \mu\text{m}$, suitable for connection of sensors. In contrast, extrusion printing of viscous pastes, while similar in concept to inkjet printing, allows more material

to be deposited more quickly to achieve resistances of a few tens of $\text{k}\Omega \text{ cm}^{-1}$ with linewidths of $200 \mu\text{m}$, suitable for powering small devices. Thus, it is clear that if resolution is of importance during fabrication then inkjet printing should be applied. However, if electrical current is of more concern then extrusion printing should be applied.

Due to the advantages of extrusion printing over inkjet printing, the former method was employed to embed tracks into a biopolymer matrix. We found that the conductivity of embedded tracks (17 S cm^{-1}) in a chitosan matrix was about 3 times higher than for tracks extruded onto glass substrates. Furthermore, SEM and EDS analyses demonstrated that extruding tracks onto chitosan substrates resulted in tracks that lie partially below the surface of the film. As a result, the conductivity of these tracks was an order of magnitude lower compared to that of embedded tracks.

We envisage that the deposition methods described here can be used to build rugged tissue-mimetic integrated structures containing conducting tracks, cells and microdevices embedded in a gel matrix.

Acknowledgements

The authors gratefully acknowledge the continued financial support from the Australian Research Council (ARC), ARC Federation Fellowship (G. G. Wallace), ARC Linkage International Fellowship (P. Calvert), ARC Future Fellowship (M. in het Panhuis) and the University of Wollongong (URC and International Travel Fund). We thank Prof. W. H. Li, Drs S. E. Moulton, M. Higgins and R. Shepherd for access to rheometer, useful discussions, atomic force microscopy, and assistance with inkjet printing, respectively.

References

- 1 M. X. Chen, *Proc. IEEE*, 2005, **93**, 1339–1347.
- 2 Y. Yoshioka and G. E. Jabbour, *Synth. Met.*, 2006, **156**, 779–783.
- 3 D.-H. Kim, M. Abidian and D. C. Martin, *J. Biomed. Mater. Res.*, 2004, **71**, 577–585.
- 4 R. A. Green, S. Baek, L. A. Poole-Warren and P. J. Martens, *Sci. Technol. Adv. Mater.*, 2010, **11**, 014107.
- 5 P. Calvert, D. Duggal, P. Patra, A. Agrawal and A. Sawhney, *Mol. Cryst. Liq. Cryst.*, 2008, **484**, 657–668.
- 6 A. Denuziere, D. Ferrier and A. Domard, *Carbohydr. Polym.*, 1996, **29**, 317–323.
- 7 S. J. Kim, K. J. Lee and S. I. Kim, *J. Appl. Polym. Sci.*, 2004, **93**, 1097–1101.
- 8 A. Schneider, L. Richert, G. Francius, J. C. Voegel and C. Picart, *Biomed. Mater.*, 2007, **2**, S45–S51.
- 9 C. Peniche, M. Fernandez, G. Rodriguez, J. Parra, J. Jimenez, A. Lopez Bravo, D. Gomez and J. San Roman, *J. Mater. Sci.: Mater. Med.*, 2007, **18**, 1719–1726.
- 10 J. Berger, M. Reist, J. M. Mayer, O. Felt and R. Gurny, *Eur. J. Pharm. Biopharm.*, 2004, **57**, 35–52.
- 11 T. Nyberg, O. Inganas and H. Jerregard, *Biomed. Microdevices*, 2002, **4**, 43–52.
- 12 J. F. Che, Y. H. Xiao, X. F. Zhu and X. J. Sun, *Polym. Int.*, 2008, **57**, 750–755.
- 13 M. Onoda, Y. Abe and K. Tada, *Thin Solid Films*, 2009, **518**, 743–749.
- 14 E. M. Thaning, M. L. M. Asplund, T. A. Nyberg, O. W. Inganas and H. von Hoist, *J. Biomed. Mater. Res., Part B*, 2010, **93**, 407–415.
- 15 J. Rhim, C. L. Weller and K. Ham, *Food Sci. Biotechnol.*, 1998, **7**(4), 263–268.
- 16 J. Rhim, S. Hong, H. Park and P. Ng, *J. Agric. Food Chem.*, 2006, **54**, 5814–5822.
- 17 K. L. Mulfort, J. Ryu and Q. Zhou, *Polymer*, 2003, **44**, 3185–3192.

-
- 18 P. Calvert and Z. Liu, *Acta Mater.*, 1998, **46**, 2565–2571.
 - 19 L. F. Deravi, A. E. Gerdon, D. E. Cliffler, D. W. Wright and J. L. Sumerel, *Appl. Phys. Lett.*, 2007, **91**, 3.
 - 20 J. L. Sumerel, L. F. Deravi, K. Sudau, J. Staton, D. W. Wright and Sis, *Displays are here to Stay: Method Development for High Throughput Process Manufacturing Methods Employing R&D Scale Ink Jet Printing*, 2007.
 - 21 H. A. Barnes, J. F. Hutton, and K. Walters, *An Introduction to Rheology*, Elsevier, Amsterdam, 1989.
 - 22 K. Osaki, T. Inoue, T. Uematsu and Y. Yamashita, *J. Polym. Sci., Part B: Polym. Phys.*, 2002, **40**, 1038–1045.
 - 23 C. J. Ferris and M. in het Panhuis, *Soft Matter*, 2009, **5**, 1466–1473.
 - 24 J. Boge, L. J. Sweetman, M. in het Panhuis and S. F. Ralph, *J. Mater. Chem.*, 2009, **19**, 9131–9140.
 - 25 B. L. Groenendaal, F. Jonas, D. Freitag, H. Pielartzik and J. R. Reynolds, *Adv. Mater.*, 2000, **12**, 481–494.
 - 26 B. Y. Ouyang, C. W. Chi, F. C. Chen, Q. F. Xi and Y. Yang, *Adv. Funct. Mater.*, 2005, **15**, 203–208.
 - 27 Y. J. Lin, F. M. Yang, C. Y. Huang, W. Y. Chou, J. Chang and Y. C. Lien, *Appl. Phys. Lett.*, 2007, **91**, 3.
 - 28 J. Y. Kim, J. H. Jung, D. E. Lee and J. Joo, *Synth. Met.*, 2002, **126**, 311–316.
 - 29 O. P. Dimitriev, D. A. Grinko, Y. V. Noskov, N. A. Ogurtsov and A. A. Pud, *Synth. Met.*, 2009, **159**, 2237–2239.
 - 30 K. J. Gilmore, M. Kita, Y. Han, A. Gelmi, M. J. Higgins, S. E. Moulton, G. M. Clark, R. Kapsa and G. G. Wallace, *Biomaterials*, 2009, **30**, 5292–5304.
 - 31 J. M. Razal, M. Kita, A. F. Quigley, E. Kennedy, S. E. Moulton, R. M. I. Kapsa, G. M. Clark and C. G. Wallace, *Adv. Funct. Mater.*, 2009, **19**, 3381–3388.
 - 32 C. J. Ferris and M. in het Panhuis, *Soft Matter*, 2009, **5**, 3430–3437.